J Mater Sci (2009) 44:1909–1917
DOI 10.1007/s10853-008-3079-y

INTERFACE SCIENCE

Dislocation boundaries in drawn single crystal copper wires produced by Ohno continuous casting

J. Chen · W. Yan · R. G. Ding · X. H. Fan

Received: 19 July 2008 / Accepted: 21 October 2008 / Published online: 11 December 2008
© Springer Science+Business Media, LLC 2008

Abstract Dislocation boundaries in drawn single-crystal copper wires produced by Ohno continuous casting have been studied via electron backscattering diffraction and transmission electron microscopy. In the undeformed wires, there are subgrains with misorientation angle lower than 4.2°. For the cold-drawn wires, we measured misorientation angle and spatial distribution of dislocation boundaries, analysing the formation mechanism of dislocation boundaries parallel to drawing direction. Regarding spatial distribution of high-angle dislocation boundaries, at the strains more than 2.77, the boundaries spread from the centre to the surface regions with increasing strain. Regarding the angular distribution of dislocation boundary misorientation, at the strain lower than 2.77, there is one peak lower than 5°. Increasing the strain to 4.12, a bimodal distribution of misorientation angles is observed. One is lower than 5°, and the other is between 45 and 50°. For dislocation boundaries parallel to drawing direction, although at low strains there are different deformation bands with different microstructures, at high strain the microstructures are characterized as dislocation boundaries parallel to drawing direction formed by two approaches: the interaction between two kinds of boundaries and the increase in misorientation angle of boundaries shared by some dislocation cells.

J. Chen · W. Yan (✉)
Department of Applied Physics, Northwestern Polytechical University, Xi'an 710072, China
e-mail: yanwen@xatu.edu.cn

J. Chen · W. Yan · X. H. Fan
School of Materials Science and Chemical Engineering, Xi'an Technological University, Xi'an 710032, China
e-mail: xatuchenjian@yahoo.com.cn

X. H. Fan
e-mail: fanxh2002@xatu.edu.cn

R. G. Ding
Department of Metallurgy and Materials, University of Birmingham, Birmingham B15 2TT, UK
e-mail: r.ding@bham.ac.uk

Introduction

Ohno continuous casting (OCC) technique is a combination of advanced directional solidification and high efficiency continuous casting, which can be used to produce unlimited lengths of single-crystal copper wires [1–5]. With almost no grain boundaries, the single-crystal copper wires show excellent capabilities for signal transmission and plastic deformation. It is found that the resistivity of single-crystal copper wires is about 15% lower and the elongation rate is about 80.24% higher than those of common copper wires [4]. Thus, single-crystal copper wires produced by OCC have become very attractive.

Up to now, technological parameters for preparing single-crystal copper wires by OCC have been identified [4]. However, since the diameter of such wires is too large for some commercial copper cables, they have to be heavily cold drawn to very fine wires. Cold-drawing makes the microstructures heavily deformed, thus affecting the properties of the wires. For example, for cables consist of drawn single-crystal copper wires, there is a directional difference of electrical signal transmission as reported by Audioquest Company [6]. Thus, for a satisfactory explanation of properties of drawn single-crystal copper wires produced by OCC method, it is necessary to systematically investigate the deformation microstructures. Whereas the

deformation microstructure following rolling, tension, and torsion has been studied widely [7–15], a study of the effect of cold-drawing on the microstructure of single-crystal copper wires has not been reported. For medium to high stacking fault energy metals processed under conditions where the plastic deformation takes place predominantly by slip [7–16], dislocation boundaries are the main features of the deformed microstructures. The present study, therefore, concentrates on analysing via electron back-scattering diffraction (EBSD) and transmission electron microscopy (TEM) dislocation boundaries in single-crystal copper wires subjected to cold-drawing.

Experimental

Single-crystal copper wires with 8 mm in diameter were produced by OCC technique. The wires were drawn at room temperature to different diameters. The drawing directions were kept the same in every time of drawing to exclude the influence of drawing direction on the deformation microstructure.

Samples for EBSD were cut according to Fig. 1. The samples were polished mechanically, and then electropolished in a solution of 500 mL distilled water, 250 mL HPO_3, 250 mL ethanol, 50 mL propanal, and 5 g carbamide at 4 V and −15 °C for 4 min. EBSD analysis was performed in a JSM-6460 scanning electron microscope (SEM) with INCA Crystal EBSD software or an FEI Nova NanoSEM 400 with HKL Channel 5 system at 20 kV. The results were analysed from the centre to the surface of the samples only due to the axial symmetry of the microstructures.

Samples for TEM were electropolished. TEM analysis was carried out on a JEM 2010 or a Tecnai 20 with acceleration voltage of 200 kV. The drawing direction that shown in Fig. 1 was made coincident with the longitudinal axis of the double-tilt specimen holder.

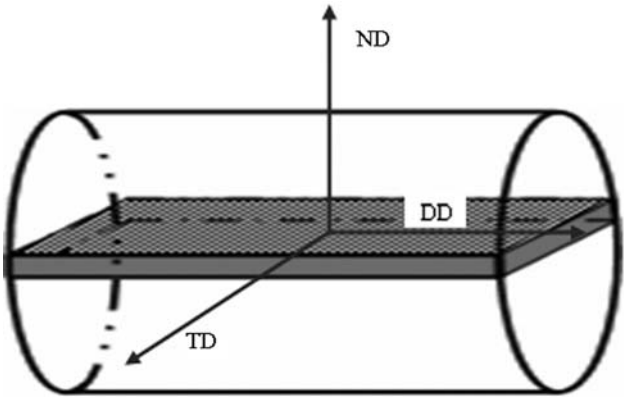

Fig. 1 Sketch of analysis samples cut from single crystal copper wires. *ND* normal direction; *DD* drawing direction; *TD* transverse direction

Results

Undeformed single crystal copper wires

Figure 2a and b shows the crystal orientation maps of undeformed samples obtained by EBSD. In Fig. 2a and b, the crystal directions indicated by colour are parallel to the drawing and transverse directions of the wires (see Fig. 1), respectively. The colours of the orientation maps correspond to the key in Fig. 2e. From Fig. 2a, it can be found that the drawing direction of single crystal copper wires is parallel to ⟨100⟩, as determined by OCC process. In the initial solidification stage of OCC, there is a competitive growth of grains due to convex solid/liquid interfaces. The grains' competition growth means that those grains with a high angle between ⟨100⟩ and the direction of heat flow, the axial direction of the wires, will be swallowed by those

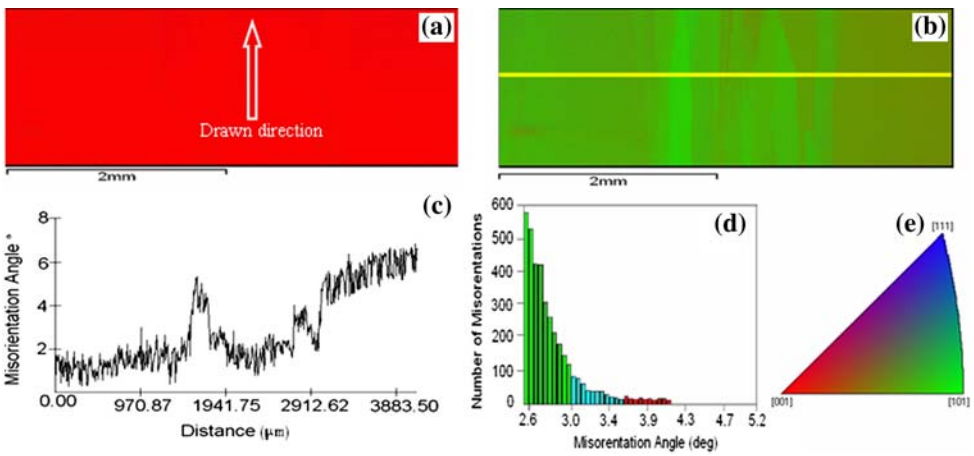

Fig. 2 Orientation maps and misorientation for longitudinal section samples of undeformed single crystal copper wires with 8 mm diameter. **a** and **b** refer to the drawing direction and the transverse direction in Fig. 1, respectively. **c** Variation in misorientation angle relating to the first point along the centre line indicated in (**b**). **d** Misorientation distribution histogram. **e** A colour key

with a low angle. Thus, the axial direction of the single crystal copper wires will be parallel to ⟨100⟩.

From Fig. 2b, it can be seen that there is a change of colours, indicating that though the axial direction of the wires is ⟨100⟩, there is the presence of misorientations. Soda et al. [3] used electron channelling contrast and Läue X-ray back-reflection to study the effect of casting speed on the quality of single crystal copper made by OCC. They also found the existence of subgrains and suggested the formation of misorientations due to high casting speed. However, in their work, the misorientation angle could not be determined by electron channelling contrast and Läue back-reflection. Figure 2c shows the variation in misorientation angle relating to the first point along the centre line indicated in Fig. 2b. Figure 2d shows the misorientation distribution histogram, indicating that the maximum misorientation angle in single crystal copper wires is <4.2° and that most of the misorientation angles are <3°.

Deformed single crystal copper wires

Microtexture and spatial distribution of dislocation boundaries

Figure 3 shows the orientation maps of drawn single crystal copper wires with different strains. In Fig. 3a–d, the crystal directions indicated by colour are parallel to the drawing direction of the wires (see Fig. 1). The colours of the orientation maps correspond to the key in Fig. 3e. From Fig. 3, it can be seen that at strains lower than 2.77, most of the fibre texture component is ⟨100⟩, which is parallel to the drawn direction. When the strain is 2.77, there is a large number of regions with a ⟨111⟩ fibre texture component parallel to the drawn direction in the centre of the wires. Increasing the strain to 4.12, the ⟨111⟩ fibre texture component in the surface and the middle regions increases comparing to the specimens with a strain of 2.77. Above analysis indicates that there is an inhomogeneous distribution of fibre texture in the wires with strains more than 2.77.

In Fig. 3, the black lines represent the dislocation boundaries with a misorientation angle more than 15°, indicating that at a strain of 2.77, the number of high-angle boundaries in the central regions is more than that in the middle and the surface regions (see Fig. 3c). When the strain is increased to 4.12, the number of high-angle boundaries in the surface and middle regions increases in comparison with the specimens with a strain of 2.77 (see Fig. 3c, d). However, when the strain is lower than 1.96, an inhomogeneous distribution of dislocation boundaries in the wires along radial direction cannot be observed, as shown in Fig. 3a, b.

Misorientation angle across dislocation boundaries

Figure 4 shows the results of line-scans from the surface to the centre of these samples with different strains, indicating that the larger the strain, the higher the proportion of high-angle boundaries. For example, when the true strain is 0.94, most of the dislocation boundaries are low angle (<15°), and the highest misorientation angle is about 30° (see Fig. 4a). However, when the strain is increased to 4.12, the number of high-angle boundaries increases and the highest misorientation angle is about 62° (see Fig. 4d).

Figure 5 shows the misorientation angle distribution of dislocation boundaries from these samples. From Fig. 5, it can be seen that when the strain is lower than 2.77, there is one peak in a range lower than 5° (as seen in Fig. 5a–c). Increased strain to 4.12, a bimodal distribution of misorientation angles is observed: one is in a range lower than 5° and the other is between 45 and 50° (as shown in Fig. 5d).

Structural morphology

From Fig. 3, it can be found that grain subdivision takes place in the wires with low strains and two kinds of deformation bands can be observed: one begins to evolve from ⟨100⟩ to ⟨111⟩ parallel to the drawn direction, and the other is still ⟨100⟩. Figure 6 shows the microstructures of drawn single crystal copper wires with different strains by

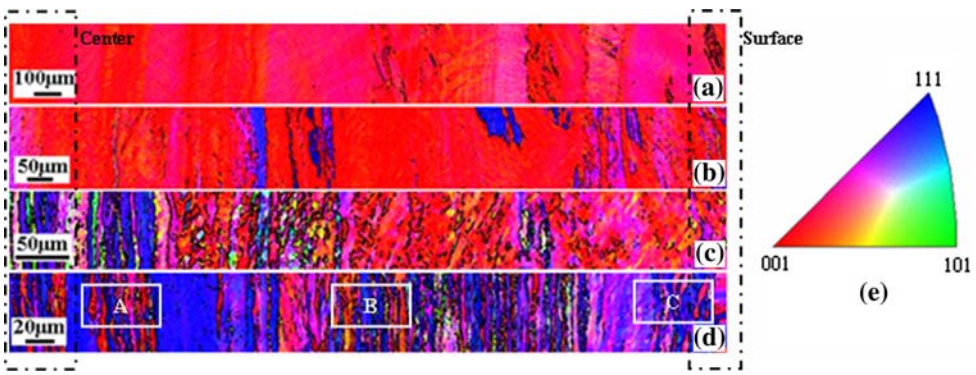

Fig. 3 Orientation maps of drawn single crystal copper wires with strains of **a** 0.94, **b** 1.96, **c** 2.77 and **d** 4.12 referred to the drawing direction. **e** A colour key. In **a–d**, *black lines* mark boundaries with a misorentation angle of more than 15°

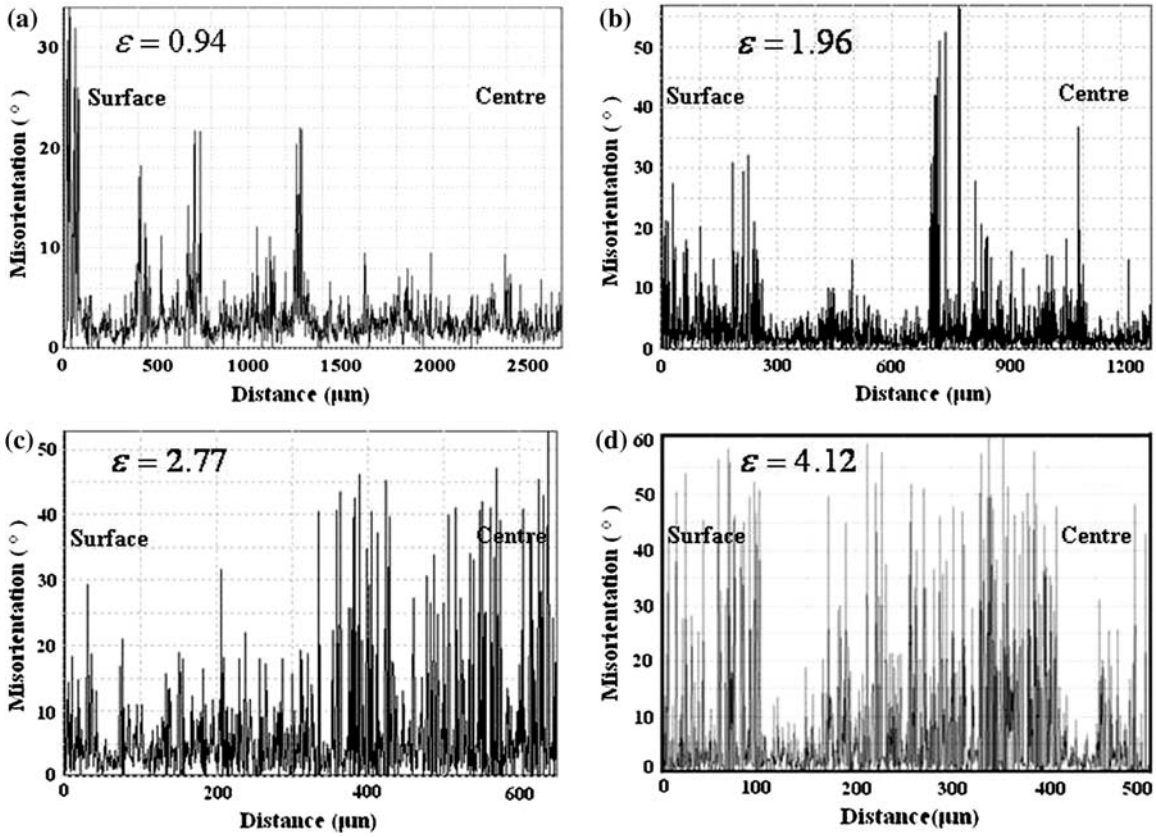

Fig. 4 Adjacent point misorientation angles versus distance along radial direction of drawn single crystal copper wires with different strains

EBSD. In Fig. 6a and b, the colours of orientation maps correspond to the key in Fig. 2e. In Fig. 6c–e, the black lines represent boundaries with a misorientation angle $>1.5°$ and the colours of orientation maps correspond to the key in Fig. 3e. From Fig. 6, it can be found that when a strain is low, there are two kinds of boundaries in the deformation bands with the drawn direction beginning to evolve from ⟨100⟩ to ⟨111⟩ (see Fig. 6b and regions denoted by "A" in Fig. 6a). Figure 7 shows the microstructures of regions with two kinds of boundaries in the wires with a strain of 0.94 by TEM, and the drawn direction in Fig. 7 is near ⟨112⟩, indicating that two kinds of boundaries are located on {111} planes and few S-bands can be seen. Figure 7b shows the microstructure of regions denoted by "A" in Fig. 7a. From Fig. 7b, we can find that there are equiaxed dislocation cells between the boundaries. Figure 8 shows the microstructures with strains of 1.96 and 2.77 in deformation bands with drawn direction beginning to evolve from ⟨100⟩ to ⟨111⟩. From Fig. 8, it can be seen that at a strain of 1.96, a part of boundaries are parallel to the drawn direction (see Fig. 8a) and when the strain is 2.77, all the boundaries are parallel to the drawn direction (see Fig. 8b).

For the deformation bands with drawn direction parallel to ⟨100⟩, EBSD results show that there are almost no boundaries in drawn single crystal copper wires with low strains (see regions denoted by "B" in Fig. 6a). Actually, during TEM analysis process, the regions with drawing direction parallel to ⟨100⟩ can also be observed in the wires with low strains, as shown in Figs. 9 and 10. From Figs. 9 and 10a, it can be found that there are few microbands (see Fig. 9) or dense dislocation walls (see Fig. 10a) and a large number of dislocation cells, and some dislocation cells share a boundary parallel to the drawing direction. Because the angular resolution of TEM is higher than that of EBSD and at low strains, the misorientation angle of dislocation cell boundaries is low, the dislocation cell boundaries may not be observed by EBSD. Figure 10c shows the microstructures in a section perpendicular to the drawn direction and the beam direction is near ⟨100⟩, indicating that the diameter of the equiaxed dislocation cells is about 0.25 μm and corresponds to that in Fig. 10a and b. Therefore, from Fig. 10a–c, it can be concluded that there are cylindrical dislocation cells elongated along the drawn direction in the deformation bands with drawn direction near ⟨100⟩. Figure 10d shows the microstructures with a strain of 4.12 in the deformation bands with drawn direction parallel to ⟨100⟩, and the width of boundaries parallel to drawing direction decreases in comparison with that at a strain of 1.96 (see Fig. 10a–c).

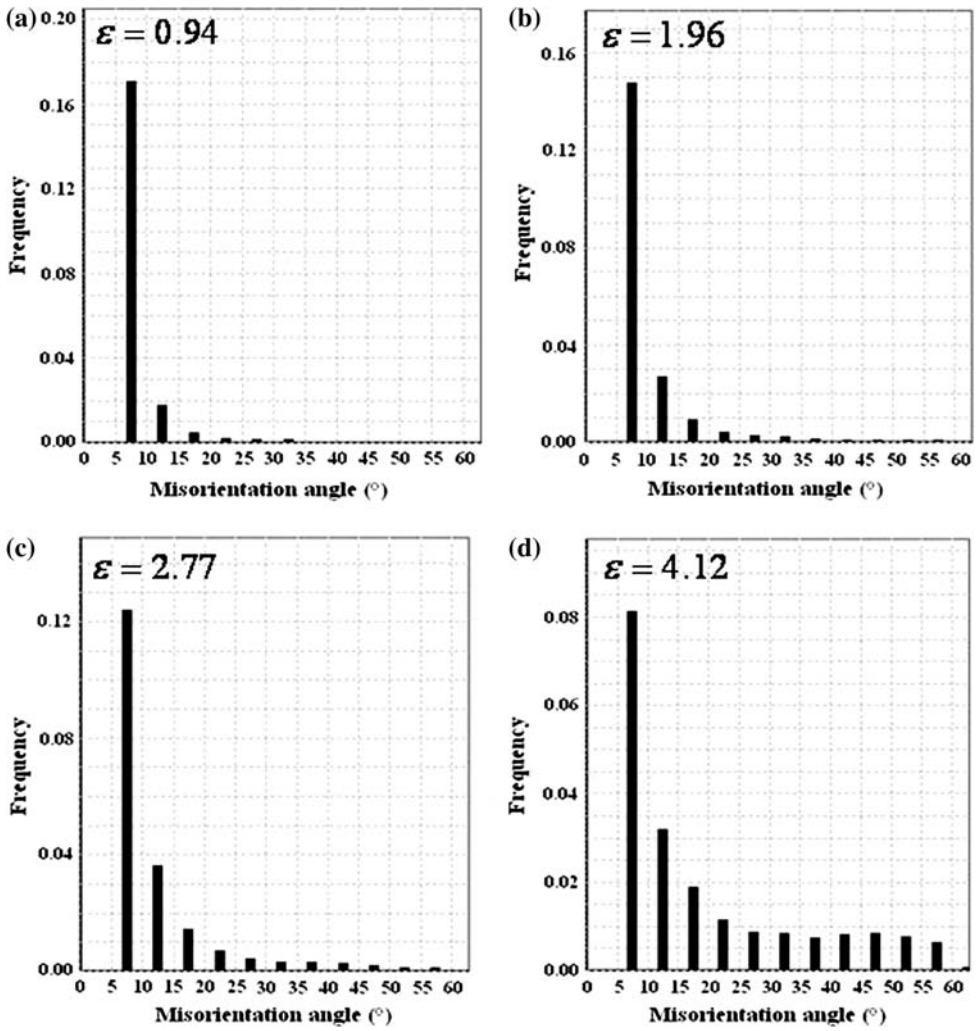

Fig. 5 Histograms of misorientation angle distribution in drawn single crystal copper wires with different strains

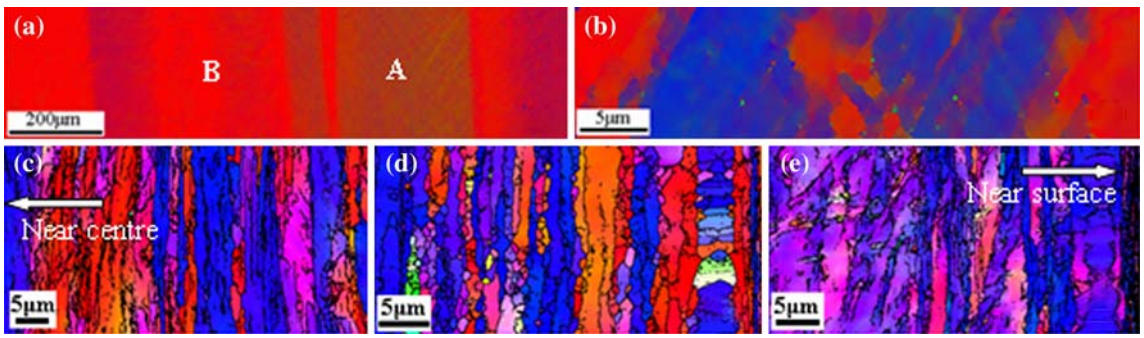

Fig. 6 Orientation maps of the wires with strains of 0.94 (**a**), 1.39 (**b**) and 4.12 (**c**–**e**) referred to the drawing direction. In (**b**) and regions denoted by "A" in (**a**), there are two kinds of boundaries. In the regions denoted by "B" in (**a**), there are almost no boundaries. In (**c**–**e**), *black lines* mark boundaries with a misorentation angle of >1.5°. **c**–**e** Correspond to the regions denoted "A", "B" and "C" in Fig. 3d, respectively. In (**a**) and (**b**), the colours of orientation maps correspond to the key in Fig. 2e, and those in (**c**–**e**) correspond to the key in Fig. 3e

Therefore, it can be concluded that although there are two deformation bands with different microstructures in the wires with low strains, when the strain is large, the microstructures can be characterized as the boundaries parallel to the drawn direction, as shown in Figs. 6c–e, 8b and 10d. At the left of Fig. 6e, a large number of boundaries parallel to the drawn direction can be observed, which may be caused by local shear during the cold-drawn processing.

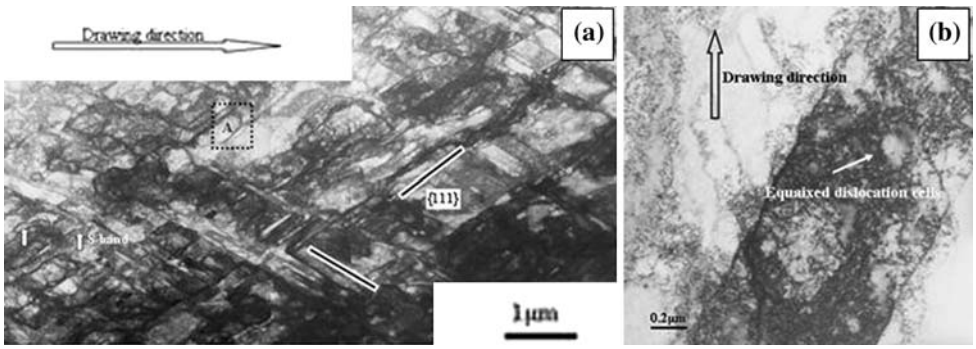

Fig. 7 Microstructures with two kinds of boundaries in the wires with a strain of 0.94. The drawn direction is near ⟨112⟩. In (**a**), two kinds of boundaries can be seen. **b** Dislocation cells in regions denoted "A" in (**a**)

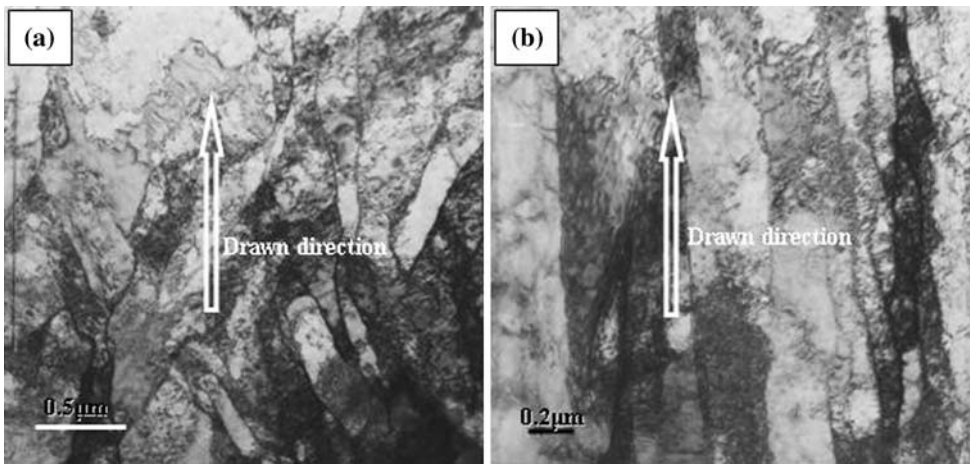

Fig. 8 Microstructures with strains of 1.96 (**a**) and 2.77 (**b**). In (**a**) and (**b**), the drawn directions are near ⟨112⟩ and ⟨111⟩, respectively

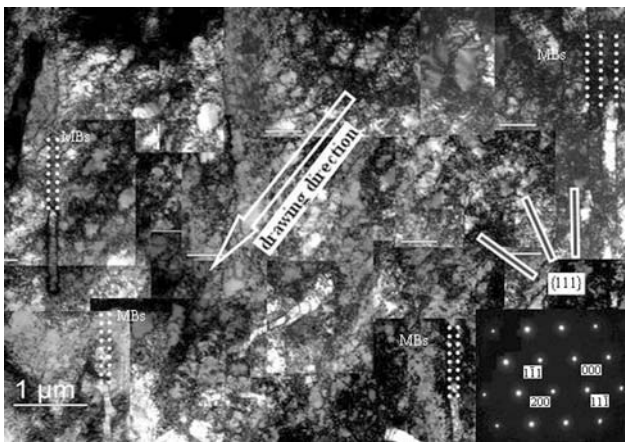

Fig. 9 Dislocation cells and a small number of microbands (MBs) in drawn single crystal copper wires with a strain of 0.94. The drawn direction is near ⟨100⟩

Discussion

Spatial distribution of textures and dislocation boundaries

For texture evolution in the cold-drawn process, many studies [16–18] proved that in polycrystalline copper wires, before recrystallization, the intensity of ⟨111⟩ fibre texture parallel to drawn direction increases with increasing strain, whereas the intensity of ⟨100⟩ decreases. ⟨111⟩ is suggested to be a stable end texture in drawn copper wires. Therefore, for single crystal copper wires with axial direction parallel to ⟨100⟩, the texture transformation process is the increase in ⟨111⟩ evolved from ⟨100⟩.

In addition to the increase in ⟨111⟩ intensity with strains increasing in the drawn single copper wires, there is inhomogeneous distribution of ⟨111⟩ texture and dislocation boundaries with high misorientation angle from the centre to the surface regions. Actually, Abdellaoui et al. [19] also studied inhomogeneous deformation resulting from drawn process, and found that the texture transition and the increase in microhardness begin at the core of polycrystalline steel wires and spread from the middle to the surface regions. According to these results, they thought that during cold-drawn process, plastic deformation begins in the central regions and when the core is not able to deform further, the deformation spreads from the centre to the surface regions.

One significant difference exists, however, comparison with the previous studies. For the single copper wires by OCC, this inhomogeneous deformation phenomenon can be observed only when the strain is more than 2.77, which may result from that there are almost no grain boundaries in the wires.

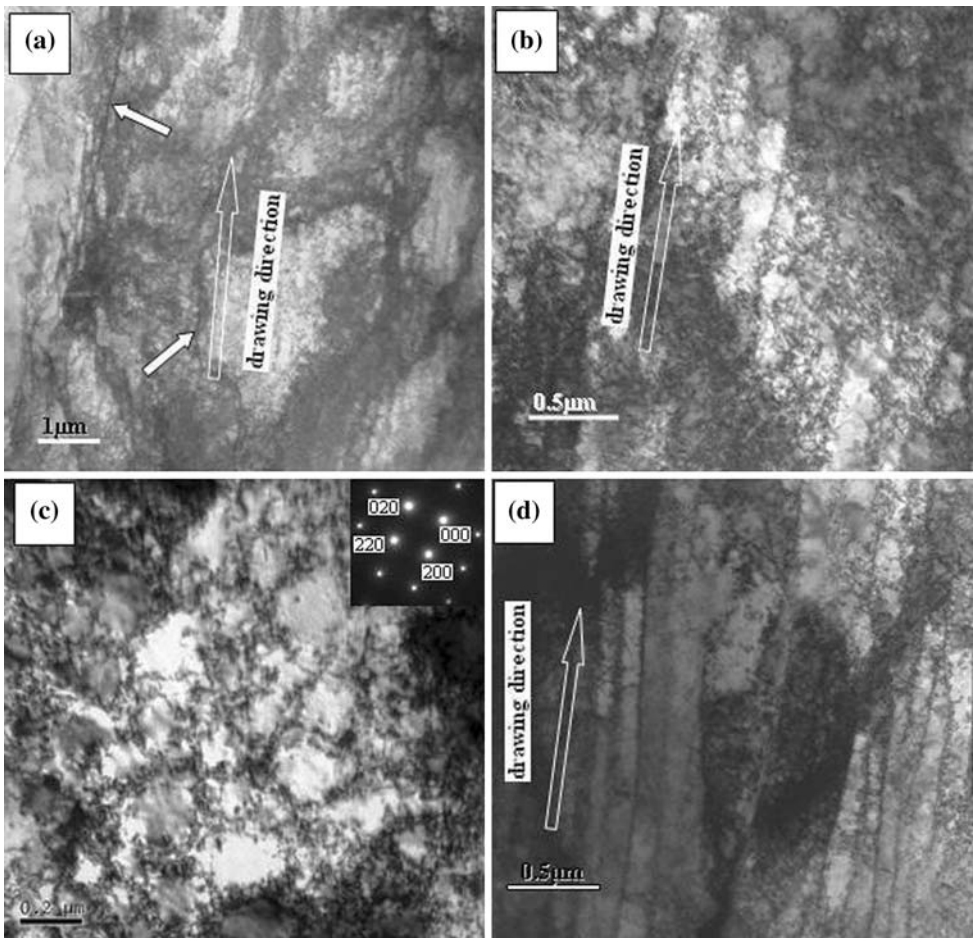

Fig. 10 Dislocation cells in drawn single copper wires with a strain of 1.96 (**a**–**c**) and lamellar boundaries in the wires with a strain of 4.12 (**c**). The drawn direction is near ⟨100⟩. **a**, **b** and **d** are the longitudinal images of drawn single copper wires. **c** The transverse image and when *X* tilt and *Y* tilt of double-tilt specimen holder are 1.9 and 0.5°, respectively, the diffraction pattern from (**c**) is at right-top of (**c**). In (**a**), the dense dislocation walls are arrowed

Misorientation angle distribution of dislocation boundaries

It has been known [20] that the dislocation boundaries resulting from deformation have a large angular spread. In cold-rolled and torsion metal, Hughes et al. [20, 21] found that when a strain is low, there is one peak in a range of low angle in the misorientation angle distribution of dislocation boundaries, whereas at large strain, a bimodal distribution of misorientation angles can be observed. It is accepted [20] that the formation of high-angle boundaries results from microstructure evolution and texture transformation. The mechanisms of microstructure evolution include cell formation, coarse slip in S-bands, coalescence of boundaries, etc. Texture mechanisms include the rotation of a subdivided grain into different preferred crystal orientations during deformation and the ambiguity of slip systems for grains with unstable crystal orientations that lead to diverging rotations within a grain. Usually, the creation of high-angle boundaries-based texture evolution will occur only after some finite deformation when the preferred end texture is well developed. In drawn single crystal copper wires with stains between 0.94 and 2.77, a large number of geometrically necessary boundaries can be observed in some regions (see Figs. 7 and 8) and the fraction of fibre texture ⟨111⟩ evolved from ⟨100⟩ is small (see Fig. 3a–c). Therefore, most of these boundaries have low misorientation angle and there is only one peak <5° in the misorientation angle distribution of dislocation boundaries (see Fig. 5a–c). However, at a strain of 4.12, a large fraction of regions with ⟨111⟩ can be observed (see Fig. 3d), and a bimodal distribution of misorientation angle appears (see Fig. 5d). Therefore, it can be concluded that most of the high-angle misorientation boundaries form by a texture mechanism in drawn single crystal copper wires.

Formation of dislocation boundaries parallel to drawing direction

In tension and cold-rolled metals with medium or high stacking fault energy [7–15, 22], geometrically necessary boundaries mainly include microbands and dense dislocation walls. When the metals are subjected to a large strain, S-bands and lamellar boundaries can form in the microstructure with planar dislocation boundary. S-bands are due to an interaction between planar dislocation boundaries and

lamellar boundaries are parallel to macroscopic deformation directions and appear after a large mount of S-bands form. The formation of geometrically necessary boundaries is considered to be closely associated with the active slip systems as determined by stress and crystal orientation. Huang and co-authors [23–26] studied the effect of grain orientation on the tension microstructures of aluminium and copper. They found that the structure with planar dislocation boundary formed in all cases except for ⟨100⟩ crystals (⟨100⟩ parallel to tension direction) in which only an equiaxed cell structure was developed.

For drawn deformation, the stress is more complex than in tension and there is shear strain [27, 28]. When the single crystal copper wires are drawn, the macroscopic subdivision of grains takes place, and two kinds of deformation bands form: one is the drawn direction of the deformation bands beginning to evolve from ⟨100⟩ to ⟨111⟩, and the other is still ⟨100⟩ (see Fig. 3a). For the former, the microstructures can be characterized as two kinds of planar dislocation boundaries not parallel to the drawn direction (see Figs. 6b and 7 and regions denoted by "A" in Fig. 6a), which is consistent with that in the microstructure deformed by tension [23–26] where the tension direction is not parallel to ⟨100⟩. At the intersection of the two kinds of boundaries, S-bands associated with shear deformation are observed and part of the shear deformation is parallel to the drawn direction (arrowed in Fig. 7). Then, if the regions with S-bands are deformed further, the lamellar boundaries parallel to drawing direction form (see Figs. 6c–e and 8).

Regarding of the deformation bands with ⟨100⟩ parallel to drawn direction in the drawn single crystal copper wires, the microstructures are characterized as some dislocation cells sharing a boundary parallel to drawn direction (see Figs. 9 and 10). In the deformation bands, because two kinds of boundaries cannot be observed, the dislocation boundaries parallel to drawing direction cannot form by the use of the mechanism mentioned above. Actually, the microstructures, which is some dislocation cells sharing a boundary parallel to drawn direction, are also observed by Wrobel et al. [29] in the cold-rolled copper of cubic orientation and Huang and co-authors [23–26], Mughrabi et al. [30] and Kawasaki and Takeuchi [31] in tensile copper and aluminium with ⟨100⟩ parallel to tensile direction. With increasing strain, the width of dislocation boundaries parallel to drawing direction decreases (see Fig. 10) and the misorientation angle of boundaries shared by dislocation cells will increase. In the deformation bands, dislocations boundaries parallel to drawn direction at a large strain may be the shared boundaries at low strains. Therefore, in drawn single crystal copper wires, although at low strain there are different deformation bands with different microstructures, the microstructures at high strain could be characterized as dislocation boundaries parallel to drawing direction formed by the above two approaches in all orientations.

Conclusions

Based on a systematic study of the dislocation boundaries in cold-drawn single crystal copper wires produced by OCC, the following conclusions can be achieved:

1. The axial direction of single crystal copper wires is parallel to ⟨100⟩, and there are subgrains with misorientations angle up to 4.2°.
2. When the strain is more than 2.77, there is an inhomogeneous distribution of fibre texture ⟨111⟩ and dislocation boundaries with high misorientation angle. With increasing strain, ⟨111⟩ fibre texture and the dislocation boundaries with high misorientation angle spread from the centre to the surface regions.
3. With increasing strain, the number of high-angle boundaries increases. The formation of high-angle boundaries mainly results from texture transformation. When the strain is 4.12, there is a bimodal distribution of misorientation angle. One is below 5° and the other is between 45 and 50°.
4. Although at low strain there are different deformation bands with different microstructures, at high strain the microstructures are characterized as dislocation boundaries parallel drawing direction formed by two approaches: the interaction between two kinds of boundaries and the increase in misorientation angle across boundaries shared by some dislocation cells.

Acknowledgements Prof. I·P. Jones (Department of Metallurgy and Materials, Birmingham University, UK) is thanked for the help of the manuscript and useful conversations. Prof. Q. Liu (Chongqing University, PR China) is thanked for help with EBSD. This study was supported by the Natural Science Foundation of China under contracts no. 50471098 and 50771076 and the Education Department Foundation of Shaanxi Province, China, under contract No. 07JK274.

References

1. Ohno A (1986) J Met 38:14
2. Yan W, Chen J, Fan XH (2003) Trans Nonferrous Met Soc China 13:1075
3. Soda H, Mclean A, Wang Z, Motoyasu G (1995) J Mater Sci 30:5438. doi:10.1007/BF00351555
4. Xu ZM, Li JG, Fu HZ (1998) Trans Nonferrous Met Soc China 8:277
5. Xu ZM, Guo ZQ, Li JG (2004) Mater Charact 53:395
6. http://www.multi-room.com/downloads/AQ/aq_cable_theory.pdf
7. Li BL, Godfrey A, Meng QC, Liu Q, Hansen N (2004) Acta Mater 52:1069
8. Hansen N (1990) Mater Sci Technol 6:1039

9. Kuhlmann-Wilsdorf D (1989) Mater Sci Eng A 113:1
10. Blicharski M, Dymek S, WrÓbel M (1995) J Mater Process Technol 53:75
11. Hughes DA, Hansen N (1993) Metall Trans A 24:2021
12. Jakobsen B, Poulsen HF, Lienert U, Almer J, Shastri SD, Sørensen HO, Gundlach C, Pantleon W (2006) Science 312:889
13. Huang X (2007) J Mater Sci 42:1577. doi:10.1007/s10853-006-0988-5
14. Huang X, Tsuji N, Hansen N, Minamino Y (2003) Mater Sci Eng A 340:265
15. Sakharova NA, Fernandes JV (2006) Mater Chem Phys 98:44
16. Waryobar DR (2003) Doctoral Thesis, The Florida State Uuniversity
17. Inakazu N, Kaneno Y, Inoue H (1994) Mater Sci Forum 157–162:715
18. Rajan K, Petkie R (1998) Mater Sci Eng A 257:185
19. Abdellaoui A, Montesin T, Heizmann JJ, Pelletier JB (1994) Mater Sci Forum 157–162:611
20. Hughes DA, Hansen N (1997) Acta Mater 45:3871
21. Hughes DA, Hansen N, Bammann DJ (2003) Scr Mater 48:147
22. Winther G (2003) Acta Mater 51:417
23. Huang X, Hansen N (1997) Scr Mater 37:1
24. Huang X, Hansen N (2004) Mater Sci Eng A 387–389:186
25. Huang X (1998) Scr Mater 38:1697
26. Huang X, Winther G (2007) Philos Mag A 87:5189
27. Li S, He S, Bael AV, Houtte PV (2004) Mater Sci Forum 408–412:439
28. Park H, Lee DN (2004) Mater Sci Forum 408–412:637
29. Wrobel M, Dymek S, Blicharski M, Gorczyca S (1994) Z MetaIlkd 85:415
30. Mughrabi H, Ungar T, Kienle W, Wilkens M (1986) Philos Mag A 53:793
31. Kawasaki Y, Takeuchi T (1980) Scr Metall 14:183